

THE GENERATION OF DIGITAL ELEVATION MODELS USING OPEN SOURCE IMAGES

by

Nithin Santosh Kumar
B.Eng., Ryerson University, Toronto, Canada, 2015

A Masters Research Project
presented to Ryerson University
in partial fulfillment of the
requirements for the degree of
Master of Engineering
in the program of
Civil Engineering

Toronto, Ontario, Canada, 2018

© Nithin Santosh Kumar, 2018

AUTHOR'S DECLARATION FOR ELECTRONIC SUBMISSION OF A MRP

I hereby declare that I am the sole author of this MRP. This is a true copy of the MRP, not including any required final revisions.

I authorize Ryerson University to lend this MRP to other institutions or individuals for the purpose of scholarly research.

I further authorize Ryerson University to reproduce this MRP by photocopying or by other means, in total or in part, at the request of other institutions or individuals for the purpose of scholarly research.

I understand that my MRP may be made electronically available to the public.

THE GENERATION OF DIGITAL ELEVATION MODELS USING OPEN SOURCE IMAGES
Master of Engineering, 2018
Nithin Santosh Kumar
Civil Engineering, Ryerson University

ABSTRACT

Digital Elevation Models are a representation of Earth's surface and are used in many areas of research. There are a number of freely available DEMs with near-global coverage, which have elevation accuracies ranging between 10 to 25 m. This project attempts to generate DEMs of comparable accuracy using open source images from satellite sensors and web mapping services. Images from Landsat 8, ASTER, and Sentinel-2 satellites, and from Microsoft's Bing Maps were used to generate DEMs for a 6.633 km² area in Oshawa, Canada. It was found that it is key that when combining images from different spaceborne sensors, the spatial resolution should be within 10 m of one another. Additionally, the radiometry of the images, in terms of intensity and contrast, must be similar. The highest accuracies of DEMs had RMSE values of 20.047 m and 20.579 m, when combining images from Sentinel-2 with ASTER and Landsat 8, respectively.

ACKNOWLEDGEMENTS

I would like to acknowledge all of the people and organizations that helped make this project possible.

I would like to thank The Airborne Sensing Corporation, and its president, Alex Giannelia, for freely providing the aerial images, associated spatial referencing, and ground control points that were used in this project. This project would not have been possible without these datasets.

I would like to thank my supervisor, Dr. Ahmed Shaker, for his guidance, input, and support throughout this project and through graduate school. I would also like to Dr. Michael Chapman, my co-supervisor, for his support through this project and graduate school as well.

I am also appreciative to the many organizations that have published the data that was used freely in this project, and for their commitment to the advancement of learning: NASA, USGS, METI, ESA, JPL, and many others.

Finally, I would like to thank my father, my mother, and Janika, whose support made this possible.

TABLE OF CONTENTS

Abstract	iii
Acknowledgments	iv
List of Tables	vi
List of Figures	vi
List of Appendices	vi
1. INTRODUCTION	1
2. STUDY AREA AND MATERIALS	2
2.1 Study Area	2
2.2 Images	2
2.2.1 Aerial Images	3
2.2.2 Landsat 8 Images	3
2.2.3 ASTER Images	5
2.2.4 Sentinel Images	6
2.2.5 Bing Maps Images	7
2.3 Ontario Ministry of Natural Resources Digital Elevation Model	8
3. METHODOLOGY	9
3.1 Image Selection	9
3.2 Preparation of Digital Elevation Models	9
3.3 Accuracy Assessment	12
3.4 Differenced Digital Elevation Models	12
4. RESULTS	13
4.1 Generated Digital Elevation Models	13
4.2 Accuracy Assessment Results	17
4.3 Differenced Digital Elevation Model Results	19
5. DISCUSSION	23
5.1 Effects of Resolution on Digital Elevation Models	23
5.2 Effects of Radiometry on Digital Elevation Models	24
6. CONCLUSION	26
APPENDIX	28
REFERENCES	34

LIST OF TABLES

Table 1 - Matrix of Possible Digital Elevation Models	10
Table 2 - Spatial Resolutions of Generated Digital Elevation Models	13
Table 3 - Accuracy Assessment Results	17

LIST OF FIGURES

Figure 1 - Study Area.....	2
Figure 2 - Landsat 8 Images.....	4
Figure 3 - ASTER Images.....	5
Figure 4 - Sentinel Image.....	6
Figure 5 - Satellite Image Footprints	7
Figure 6 - Generated Digital Elevation Models	15
Figure 7 - Differenced Digital Elevation Models	20

APPENDIX TABLE OF CONTENTS

Figure 8 - Landsat 8 Panchromatic Images.....	28
Figure 9 - Bing Maps Images.....	28
Figure 10 - Generated Digital Elevation Models, Unique Scales	29
Table 4 - Elevations at Ground Control Points	31
Figure 11 - Differenced Digital Elevation Models, Unique Scales	32

1. INTRODUCTION

A Digital Elevation Model (DEM) is a digital representation of the Earth's surface. DEMs provide information about the surface elevation and topography that is important to many areas of research, such as resource management, hydrology, and geology, among many others. Common methods of obtaining elevation data include land surveying and aerial surveying, which may be expensive options. However, there are freely available near-global DEMs that are generated using spaceborne sensors and have vertical accuracies in the magnitude of metres (Yang et al., 2016).

One freely available DEM is the Advanced Spaceborne Thermal Emission and Reflectance Radiometer Global DEM (ASTER GDEM), generated using images from the spaceborne ASTER sensor. The ASTER GDEM is reported to have vertical Root Mean Square Errors (RMSE) between 10 m and 25 m (METI, 2009). Another freely available DEM is the Shuttle Radar Topography Mission DEM (SRTM DEM), which is reported to have a vertical accuracy of 16 m (NASA, 2001). However, the SRTM DEM has at times been found to have a Root Mean Square Error (RMSE) as high as 23 m in certain areas (Li et al., 2013). Additionally, there is the Earth-Env-DEM90, which is a fusion of the ASTER and SRTM DEMs developed by Robinson et. al (2014), and has produced RMSE values of 10.55 m, with accuracies reaching 5.36 m in certain areas. Sources of errors are attributed to primary data, specifically spatial resolution of images (Sharma et al., 2011), as well as algorithms of elevation derivation (Hirt et al., 2010).

Since all that is required to derive elevation is stereo images, it is then possible that overlapping images from satellite sensors may produce DEMs. This project will attempt to generate DEMs from open source images that may act as an alternative to freely available DEMs. Open source images that will be used will be from the Landsat 8, ASTER, and Sentinel satellites. Additionally, aerial images from Microsoft's Bing Maps web mapping service will be used. These sources were chosen for their varying spatial resolutions, which was mentioned as one of the leading causes of elevation errors by Li et. al (2017), to identify the effects that resolution has on elevation.

The DEMs derived from the open source images will have their elevation accuracy assessed using ground control points established in a 6.633 km² area in Oshawa, Canada. Also, accuracy would be tested against a control DEM published by the Ontario Ministry of Natural Resources.

(Note: Digital Surface Models and DEMs are considered synonymous for this project.)

2. STUDY AREA AND MATERIALS

2.1 Study Area

The study area for the project was a section of Oshawa, Ontario, measuring 3.088 km by 2.128 km (6.633 km²), seen in Figure 1. This region was selected because aerial images and ground control points were made available for it, thanks to The Airborne Sensing Corporation. Since this was the available area for control, the project was then centred around attempting to determine the accuracy of DEM generation for areas of similar size and landcover from open source satellite images and images that may be easily obtained from web mapping sources.

In this case, the study area was residential, with the Oshawa Creek running through the centre, providing a region of lower elevation compared to the rest of the scene. Also, the South edge of the study area is approximately 3.5 km from the shore of Lake Ontario, and there is a noticeable sloping of the land toward the lake to the South, as seen in the control DEM, mentioned later on.



Figure 1 - The study area, outlined, within Oshawa, Canada

2.2 Images

Images from five sources were used for DEM generation: 1) Aerial images, 2) Landsat 8 images, 3) ASTER images, 4) a Sentinel image, and 5) images from Bing Maps. The inclusion of the satellite images was based not only on their open source nature, but also because of their varying spatial resolutions and, in certain cases, for providing stereo coverage of the study area.

For consistency, the satellite images were obtained in time frames as close to one another as possible, even though the elevation of the study area was not expected to change noticeably in even a large period of time. Since the aerial images were taken in February 2016, the satellite images were acquired in a time frame that was as close to February 2016 as possible. Constraints on obtaining images close to that time were the availability of images with minimum cloud cover as well as temporal resolution.

The aerial images were obtained from The Airborne Sensing Corporation, the satellite images were obtained from United States Geological Survey (USGS) Earth Explorer, and the Bing Maps images were obtained from <http://bing.com/maps>.

2.2.1 Aerial Images

There were ninety-two aerial images used to generate a DEM. The images were taken by The Airborne Sensing Corporation on February 22, 2016, with a Vexcel UltraCam. The exterior orientation parameters of the images were obtained using Applanix GNSS and IMU sensors. The images and associated data were collected as part of an IMU calibration flight near the company's airbase at the Oshawa Executive Airport.

The images were taken at an average flying height of 906 m above the ellipsoid, World Geodetic System 1984 (WGS84). The images have an approximate resolution of 0.07 m, and each pair of overlapping images meet a minimum standard of 60% overlap and 30% sidelap.

2.2.2 Landsat 8 Images

Two Landsat 8 images were used for DEM generation, and may be seen in Figure 2. Landsat 8 is the most recent satellite in the Landsat program, launched in February 2013, as a collaborative effort between NASA and the USGS. The satellite's "Operational Land Imager" contains a push-broom linear array sensor, which means the sensor detects pixels in an across-track line.

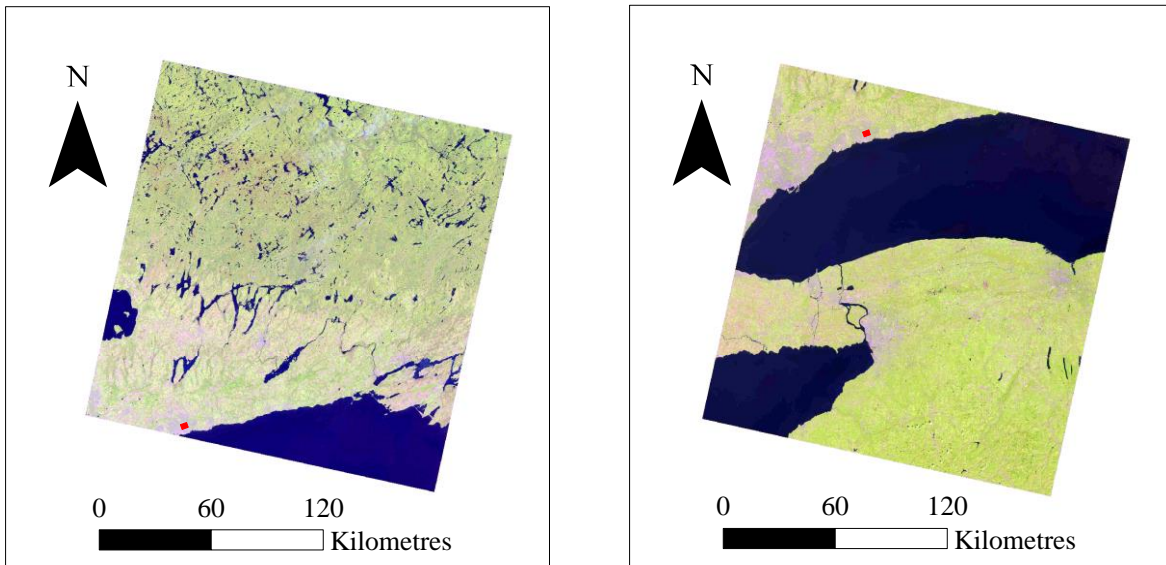


Figure 2 - Landsat 8 Multispectral-29 (left) and Landsat 8 Multispectral-30 (right), with study area is marked in red. The images are numbered for their WRS Row Number

Though the two images appear to overlap, they are not stereopairs. This is because the push-broom sensor may only capture an image from one pose, when on the same path. This means that the area of overlap was actually taken from the same pose, and that any apparent overlap may be attributed to the division of the images in post-processing. Any apparent differences seen in the overlap would be due to potential geometric and radiometric corrections applied to the images in the post-processing phase, before publication.

The study area was located in the apparent overlap of two images, for this reason, both images were included in the generation of DEMs. However, the two images may not be used with one another to create a DEM, again, because Landsat 8 contains a push-broom sensor, meaning that coincident features in both images were taken from the same camera pose.

The Landsat 8 Multispectral images that were used contain Band 2 (Blue, 0.452 – 0.512 μm), Band 3 (Green, 0.533 – 0.590 μm), and Band 4 (Red, 0.636 – 0.673 μm). The images have a spatial resolution of 30 m and were both taken from World Reference System (WRS) Path 17, and from consecutive Rows 29 and 30, on September 16, 2015. To distinguish between the two Landsat 8 images for the remainder of the report, they will be identified by their unique row number (i.e. Landsat 8 Multispectral-29 and Landsat 8 Multispectral -30).

Additionally, Band 8 (Panchromatic, 0.503 – 0.676 μm) for both images were included because the panchromatic spatial resolution is 15 m. These images will be referred to as Landsat 8 Panchromatic-29 and Landsat 8 Panchromatic-30, also in accordance with the images' unique row number. The Landsat 8 Panchromatic images may be seen in the Appendix, Figure 8.

2.2.3 ASTER Images

Two Advanced Spaceborne Thermal Emission and Reflectance Radiometer (ASTER) images were included in DEM generation, and may be seen in Figure 3. The ASTER sensor was developed by the Japanese Ministry of Economy, Trade and Industry (METI), and operates onboard the NASA Terra satellite, which was launched in December 1999. Similar to Landsat 8, the ASTER Visible Near Infrared (VNIR) sensor is a push-broom.

As mentioned earlier, ASTER images are used to create the ASTER GDEM, using images from forward and backward mounted sensors. Images from the backward-facing sensor, named Band 3B, are not freely available.

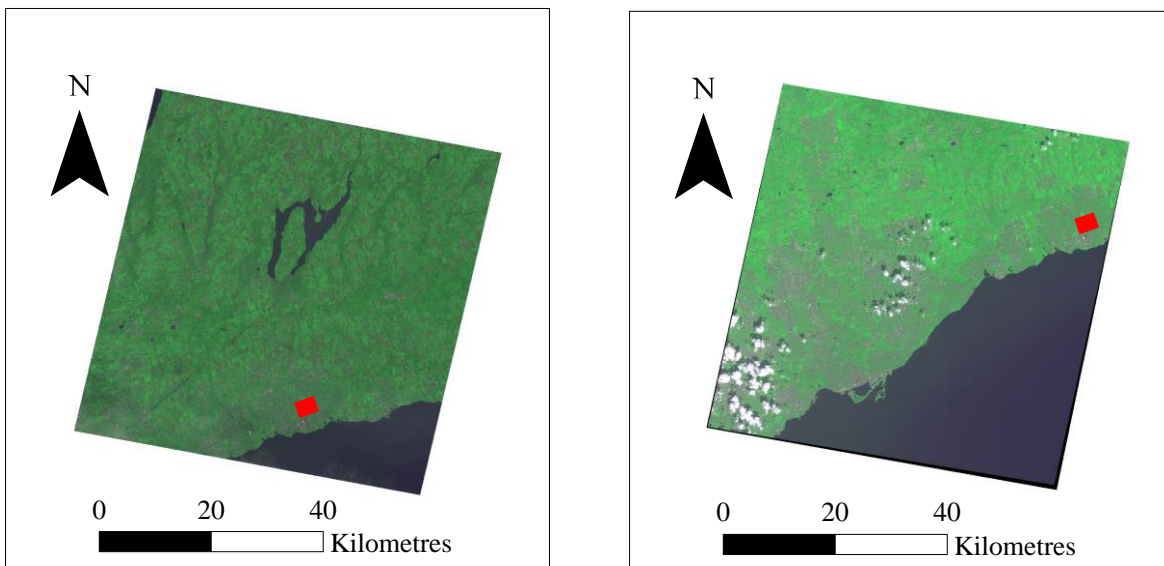


Figure 3 - ASTER-17 (left) and ASTER-18 (right), with study area is marked in red. The images are numbered for their WRS Path Number.

The two Landsat 8 images were not stereopairs because they were taken from the same path with a push-broom sensor. However, the two ASTER images are from different paths, meaning that they were taken from different poses and are, in fact, stereopairs. The images were taken from neighbouring paths 17 and 18 and share an approximate 29% overlap.

The ASTER images contain Band 1 (0.520 – 0.600 μm), Band 2 (0.630 – 0.690 μm), and Band 3N (0.780 – 0.860 μm), from the VNIR (Visible Near Infrared) subsystem. The images have a spatial resolution of 15 m, and were both taken from Row 29, and from consecutive Paths 17 and 18. The image on Path 17 was taken on September 25, 2013, and the image on Path 18 was taken on August 12, 2011. To distinguish between the two ASTER images for the remainder of the report, they will be identified by their unique Path number (i.e. ASTER-17 and ASTER-18).

2.2.4 Sentinel Images

One Sentinel image was included for DEM generation, and may be seen in Figure 4. The two Sentinel-2 satellites were launched in June 2015 and March 2017, by the European Space Agency. Similar to the previous two sensors that were discussed, the Sentinel-2 sensor is a push-broom.

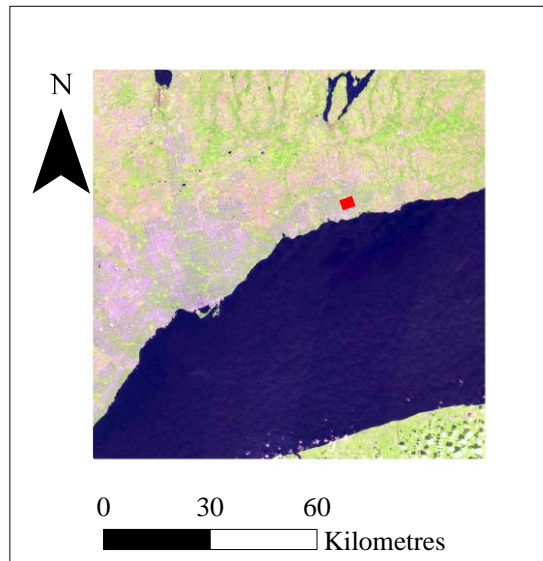


Figure 4 - The Sentinel image used, with study area is marked in red.

The image was taken on September 24, 2016. Similar to Landsat 8 and ASTER, the Sentinel sensor does not produce stereo-images, and the study area is not located in a region of overlap for Sentinel images, meaning that only one image may be used.

The Sentinel image contains Band 4 (Red, 0.635 – 695 μm), Band 3 (Green, 525 – 595 μm), and Band 2 (Blue, 0.425 – 0.555 μm). The image has a spatial resolution of 20 m.

The Sentinel image was the final satellite image included. Figure 5 illustrates the spatial coverage of the images from the satellite sensors involved in DEM generation.

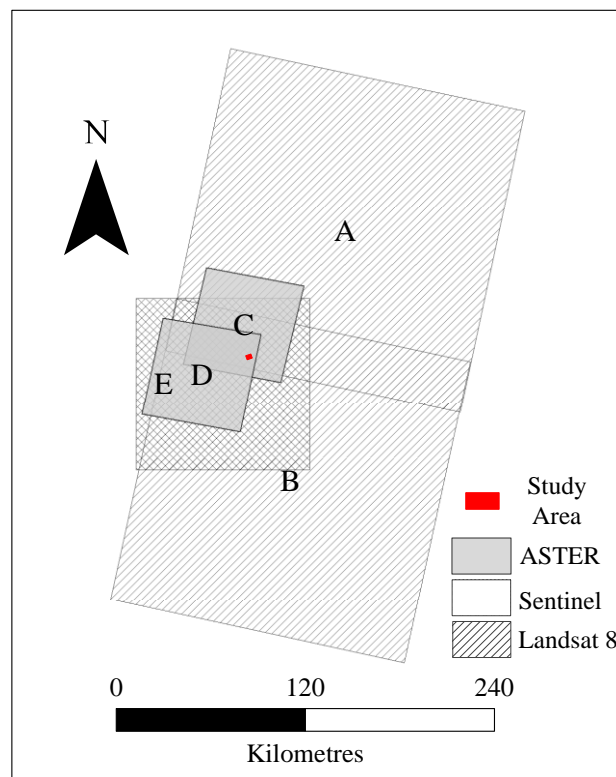


Figure 5 – Footprints of the five satellite images used. (A) represents Landsat 8-29, (B) Landsat 8-30, (C) ASTER-17, (D) ASTER-18, (E) Sentinel.

2.2.5 Bing Maps Images

A final source of open source images came from Bing Maps. Bing Maps is Microsoft Bing’s search engine web mapping service. The mapping service uses aerial imagery for visualization, which

was selected for DEM generation. The service is similar to that of web mapping services offered by Google, with the difference of using aerial images, instead of satellite images, as is the case with Google.

The resolution of the images obtained from Bing Maps were variable based on the scale that the image was displayed in, i.e. the level of zoom. For a small scale (zoomed out), the image would cover a large spatial area and be represented with the number of pixels available on the display screen, resulting in a coarse spatial resolution. However, for a large scale (zoomed in), the image would cover a small spatial area, but be displayed with the same number of pixels, resulting in a finer spatial resolution.

Because of this, images at different scales were captured for DEM generation. Images with spatial resolutions of 0.15 m, 13 m, and 27 m were obtained, and may be seen in the Appendix, Figure 9.

2.3 Ontario Ministry of Natural Resources Digital Elevation Model

To serve as a control, aside from the ground control points established in the study area, the results were also compared to a publicly available provincial DEM published by the Ontario Ministry of Natural Resources. The dataset was created using the Ontario Base Map (OBM) Contour dataset, OBM Spot Heights, and Water Virtual Flow.

The DEM is a raster dataset published on May 1, 2006, representing surface elevations with a spatial resolution of 10 m. The accuracy of this dataset is reported to be ± 5 m, vertically, and ± 10 m, horizontally.

3. METHODOLOGY

3.1 Image Selection

As discussed earlier, the open-source images selected for DEM generation were from the Landsat 8, ASTER, and Sentinel-2 satellites, and also from Bing Maps. The image sources were selected for their open source nature, and in the case of the three satellites, the open source archive of images.

Another reason for the selection of the satellite images was their near-global coverage. The three satellites have near-polar orbits, allowing for near-global coverage, additionally, Bing Maps has a full global coverage of images.

The final reason that these sources of imagery were chosen was because of their varying spatial resolution. The Landsat 8 Multispectral images have resolutions of 30 m, the Landsat 8 Panchromatic images have resolutions of 15 m, the ASTER images have resolutions of 15 m, the Sentinel image has a resolution of 20m, and finally, the Bing Maps images have varying resolutions based on the scale in which the scene is presented. This would allow for the investigation into the effects of differing resolutions on the accuracy of the resulting DEM.

3.2 Preparation of Digital Elevation Models

Once the images were selected, the possible combinations of pairs of images were considered for DEM generation. Though it was possible to have used more than two images of the study area to generate a DEM, this project considered the accuracy of DEMs created by using two images only.

Table 1 is a matrix of all potential image combinations that would be tested. The nine image sources are listed, along with their resolutions along the column and row headings. The empty intersecting cell represents a potential DEM pair. Certain cells are blacked-out to remove redundancies, and also to remove illogical pairs, such as the Landsat 8 images, because they were taken from the same path with a push-broom sensor, which, as explained earlier, results in them being unable to generate a DEM. Also, the Bing Maps images were paired with only one of each of the Landsat 8 Multispectral, Landsat 8 Panchromatic, and ASTER images. This results in a total of twenty-seven possible DEMs that may be generated.

Source		Landsat 8 Multispectral-29	Landsat 8 Multispectral-30	Landsat 8 Panchromatic-29	Landsat 8 Panchromatic-30	ASTER-17	ASTER-18	Sentinel	Bing Maps	Aerial			
	Resolution (m)	30	30	15	15	15	15	20	Var.	0.07			
Landsat 8 Multispectral-29	30												
Landsat 8 Multispectral-30	30												
Landsat 8 Panchromatic-29	15												
Landsat 8 Panchromatic-30	15												
ASTER-17	15												
ASTER-18	15												
Sentinel	20												
Bing Maps	Variable												
Aerial	0.07												

Table 1 - Matrix of the twenty-seven possible combinations of image pairs for DEM generation.

Once the possible images pairs were determined, their DEMs were generated. All of the DEMs were generated using Agisoft’s PhotoScan photogrammetry software, except for the DEM generated using the aerial images, which were done using ERDAS Imagine.

PhotoScan generates DEMs by first reading the images and any associated spatial reference. Then, it performs a feature detection process to identify tie points between the two images. The positions of the two images are then determined through a process of triangulation, allowing for the tie points to also be given spatial reference. After determining the locations of these tie points, the software then constructs a spatially-referenced “dense cloud”, which is the determination of significantly

more matched points between the two images, now that the orientation of the cameras is known. Finally, a DEM may be generated by creating an interpolated raster surface given the dense cloud.

In the process of DEM generation, PhotoScan allows the user to determine the level of accuracy with which the tie points should be selected. For consistency, and also to obtain the theoretically most accurate results, the highest level of accuracy was chosen (“Highest” accuracy tie point generation). Also, the user is allowed to select the level of quality and the level of depth filtering with which the dense cloud will be generated. Again, the highest levels of processing were selected for this project (“Ultra High” quality dense cloud generation, and “Aggressive” depth filtering).

Also, the Landsat 8 Multispectral images, ASTER images, Sentinel image, and Bing Maps images were converted to grayscale when processed in pair with either of the Landsat 8 Panchromatic images, which appear in grayscale. This is so that both images in a pair appear in grayscale when processed in PhotoScan. The software appeared to perform best when image pairs were both represented in grayscale or were both represented in RGB, but not both.

Due to the proprietary nature of Agisoft’s PhotoScan, additional information about the algorithms for feature detection, triangulation, dense cloud construction, and DEM generation is not known.

The DEM generated from the aerial images was produced in ERDAS Imagine’s Photogrammetry suite. The software follows a similar process to PhotoScan, but requires the exterior orientation of the images to be known. A pixel sampling distance of 8 pixels was selected to generate matched points between images. Though 8 points is a fairly high sampling interval, it was selected due to computational limits. The result of this sampling interval was a DEM of degraded quality. However, this was deemed acceptable for this study, since the scope is mainly to investigate the accuracy DEMs generated using open source data, of which the aerial images are not.

The results of the processes produced DEMs with the spatial coverage equal to that of the overlap of the image pair used to generate it. The DEMs were then clipped to cover only the study area in Oshawa, Ontario.

3.3 Accuracy Assessment

The accuracy of the DEMs were investigated by determining the Root Mean Square Error (RMSE) of the DEMs with respect to the twenty-five ground control points, listed in the Appendix, Table 4. Additionally, the Mean Error and Standard Deviation, was used for testing the accuracy of the DEMs (Li et al., 2017; Robinson et al., 2014; Li et. al., 2013). The RMSE and Standard Deviation values would give indications of relative error in elevation, and the Mean Error would indicate elevation bias. The formulas used are given below.

$$\text{RMSE} = \sqrt{\frac{\sum_{i=1}^n (z_i - Z_i)^2}{n}} \quad (1)$$

$$\text{Mean Error, } \bar{e} = \sqrt{\frac{\sum_{i=1}^n (z_i - Z_i)}{n}} \quad (2)$$

$$\text{Standard Deviation} = \sqrt{\frac{\sum_{i=1}^n (z_i - Z_i - \bar{e}_i)^2}{n-1}} \quad (3)$$

Where z_i is the elevation from the generated DEM at the location of the control point, Z_i is the elevation of the control point, and \bar{e} is the mean error.

3.4 Differenced Digital Elevation Models

Over a study area of 6.633 km², the twenty-five ground control points that were used may not provide a sufficient sample size. For this reason, the elevation errors associated with the DEMs were compared visually, as was performed by Rayburg et. al (2006) and Risbøl et al. (2015).

The control DEM from the Ministry of Natural Resources, represented as a raster dataset, was subtracted from the generated DEMs, also in raster format. The result was a model representing the difference in elevation from the control surface. Meaning, that by visual interpretation, the closer the value at any point in the model is to zero, then the more accurate the result is.

4. RESULTS

4.1 Generated Digital Elevation Models

The generation of DEMs for the twenty-seven possible image pairs was attempted. Of the twenty-seven potential pairs, seven DEMs were generated, and twenty image pairs failed to generate DEMs. The spatial resolutions of successfully generated DEMs are provided in Table 2, which is similar to Table 1, except with entirely blacked out columns removed.

		Resolution (m)				
Source		ASTER-17	ASTER-18	Sentinel	Bing Maps	Aerial
	Resolution (m)	15	15	20	13	0.07
Landsat 8 Multispectral-29	30	30.00	X	20.00		X
Landsat 8 Multispectral-30	30	X	X	30.04	X	X
Landsat 8 Panchromatic-29	15	X	X	X		X
Landsat 8 Panchromatic-30	15	X	X	X	X	X
ASTER-17	15			20.01		X
ASTER-18	15			20.03	15.00	X
Sentinel	20				X	X
Bing Maps	13					X
Aerial	0.07					0.74

Table 2 - Spatial resolutions of the seven generated DEMs. Crossed out cells represent image pairs that failed to be generated.

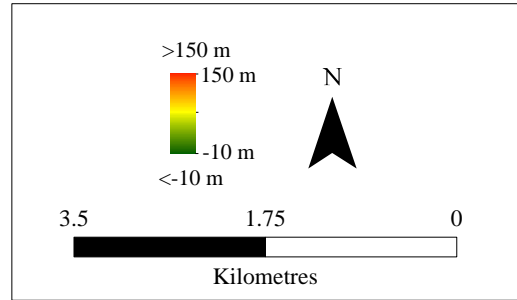
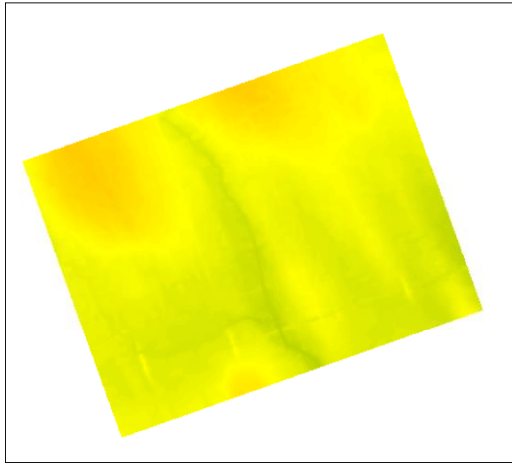
The images of various resolutions from Bing Maps failed to generate DEMs with any other image, except in the case of a 13 m resolution Bing Maps image paired with ASTER-18.

The resolutions of the resulting DEMs are relatively close to the resolutions of the images used to generate them, except in the case of the aerial image. This is due to the 8-pixel sampling interval that was chosen in processing, as discussed in the Methodology.

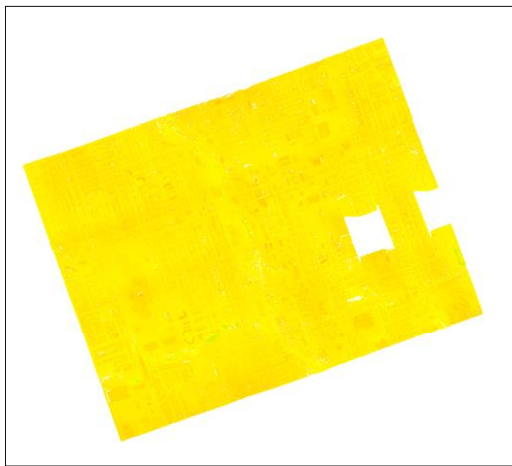
The spatial resolutions of the remaining DEMs are all close or identical to those of the image of coarser resolution in the pair used to generate them. This is the case with all, except the DEM generated using Landsat 8 Multispectral-29 and Sentinel, which has a spatial resolution of 20.00 m, identical to that of the spatial resolution of Sentinel, the image with finer resolution of the pair. In this case, the higher resolution may be attributed to a high number of points that were matched.

Besides that case, the resulting spatial resolutions are nearly those of the image with coarser resolution used to generate them. This is expected, as the feature matching algorithm would be limited to what features are detectable on the coarser image.

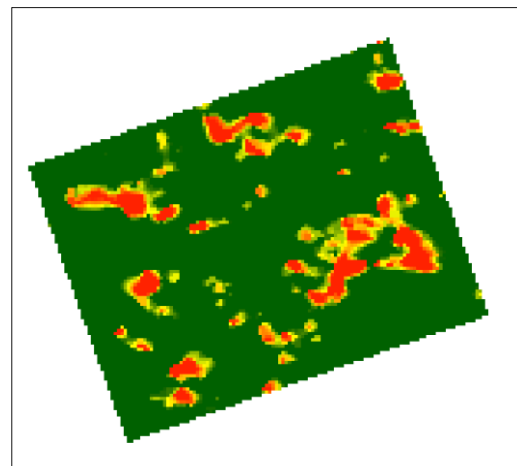
The seven DEMs that were produced, along with the control DEM from the Ministry of Natural Resources may be found in Figure 6, on the following pages. The DEMs in Figure 6 all appear in the same elevation scale, indicated at the top of the figure, along with the control DEM from the Ontario Ministry of Natural Resources. This was for the sake of comparison. (The same DEMs, represented in unique scales, based on each model's maximum and minimum elevation values may be found in the Appendix, Figure 10).



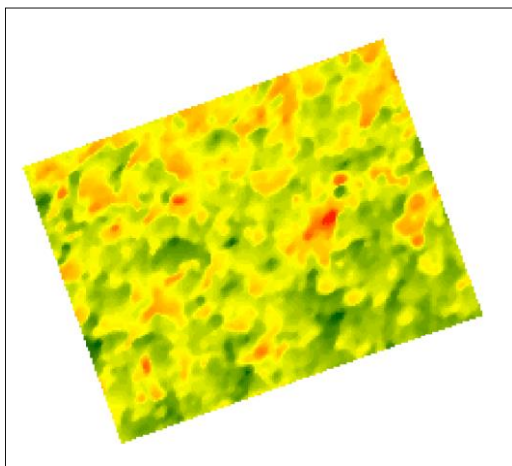
Ministry of Natural Resources (control)



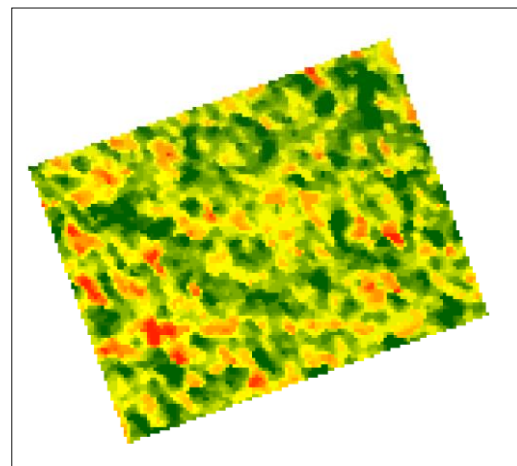
Aerial



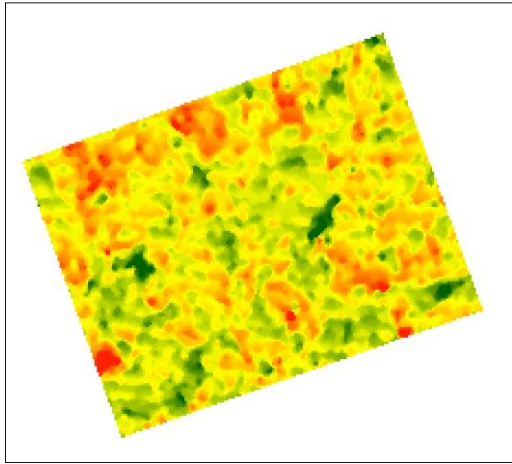
ASTER-17 and Landsat 8 Multispectral-29



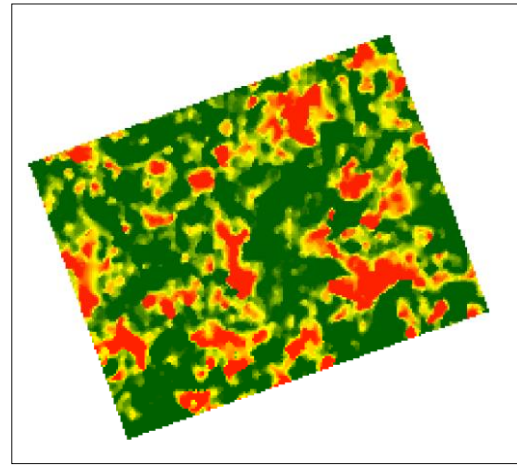
Sentinel and Landsat 8 Multispectral-29



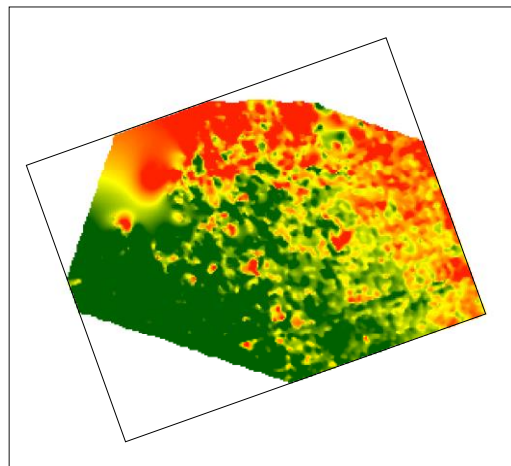
Sentinel and Landsat 8 Multispectral-30



Sentinel and ASTER-17



Sentinel and ASTER-18



ASTER-18 and Bing Maps

Figure 6 - The seven DEMs that were generated, identified by image pairs used to generate them. The DEMs are represented in the same elevation scale, indicated at the top, along with the control DEM from the Ontario Ministry of Natural Resources

It should be noted that the DEMs were all clipped to fit the study area. In the case of the DEM generated from aerial images, there were no stereopairs for certain regions, meaning that the DEM has no data in those regions. Also, in the case of the DEM generated with the images ASTER-18 and Bing Maps, PhotoScan was not able to generate tie points over the entire study area, also meaning that there are regions with no data.

4.2 Accuracy Assessment Results

The results of the accuracy assessment, represented by RMSE, Mean Error, and Standard Deviation, may be found in Table 3.

Control DEM		RMSE (m)	Mean Error (m)	Standard Deviation ($\pm m$)
Ontario Ministry of Natural Resources		4.463	-4.431	0.539
Derived DEM Image Source(s)		RMSE (m)	Mean Error (m)	Standard Deviation ($\pm m$)
Aerial		7.887	4.313	6.745
ASTER-17	Landsat 8 Multispectral-29	236.094	-190.896	141.785
Sentinel	Landsat 8 Multispectral-29	20.579	-10.680	17.954
Sentinel	Landsat 8 Multispectral-30	48.745	-24.941	42.745
Sentinel	ASTER-17	20.047	6.011	19.519
Sentinel	ASTER-18	101.327	-46.321	91.979
ASTER-18	Bing Maps	142.294	-91.189	111.806

Table 3 - RMSE, Standard Deviations, and Mean Errors of the generated and published DEMs

From Table 3, it may be seen that the accuracy assessment was also applied to the control DEM from the Ministry of Natural Resources. This was done to assess their claim that of vertical accuracy of ± 5 m. The results for the control agreed with the published claim (RMSE = 4.463 m, Standard Deviation = ± 0.539 m).

The generated DEM with the least error, as expected, was the one from the aerial images (RMSE = 7.887 m, Standard Deviation = ± 6.745 m). However, this level of error is rather high given the 0.07 m spatial resolution of the aerial images. The cause for this is attributed to the fact that lower processing standards were used in the generation of this DEM due to computational restrictions.

Of the open source image DEMs, the DEM generated from Sentinel and Landsat 8 Multispectral-29 (RMSE = 20.579 m, Standard Deviation = ± 17.954 m), and the DEM generated from Sentinel and ASTER-17 (RMSE = 20.047 m, Standard Deviation = ± 19.519 m), produced results with the least amount of error, and least amount of elevation bias (Mean Error = -10.680 m, and Mean Error = 6.011 m, respectively).

In the case of the Sentinel and ASTER-17 DEM, the RMSE of 20.047 m was generated by using 20 m and 15 m image spatial resolutions, respectively. And in the case of the Sentinel and Landsat 8 Multispectral-29 DEM, the RMSE of 20.579 m, was generated by using 20 m and 30 m spatial resolutions, respectively. This meant that the RMSE values were approximately equivalent to that of one Sentinel pixel, measuring 20 m, and significantly better than Landsat 8's 30 m pixels. This is also comparable to the ASTER GDEM accuracies.

The DEM generated with Sentinel and Landsat 8 Multispectral-30 (RMSE = 48.745 m, Standard Deviation = ± 42.745 m) and the DEM generated with Sentinel and ASTER-18 (RMSE = 101.327 m, Standard Deviation = ± 91.979 m) contained slightly greater levels of error. They produced biases of -24.941 and -46.321 m of Mean Error, respectively.

In the case of the Sentinel and Landsat 8 Multispectral-30 DEM, the RMSE of 48.745 m is equivalent to less than two 30-metre pixels from the Landsat 8 image (additionally, less than three 20-metre Sentinel pixels). And in the case of the Sentinel and ASTER-18 DEM, the RMSE of 101.327 m measured approximately five 20-metre Sentinel pixels (otherwise, approximately seven 15-metre ASTER pixels).

Finally, the DEMs produced by ASTER-17 and Landsat 8 Multispectral-29 (RMSE = 236.094 m, Standard Deviation = ± 141.785 m), and by ASTER-18 and Bing Maps (RMSE = 142.294 m, Standard Deviation = ± 111.806 m) produced the results with the most error. These DEMs also had the highest level of bias, with -190.896 m and -91.189 m, respectively.

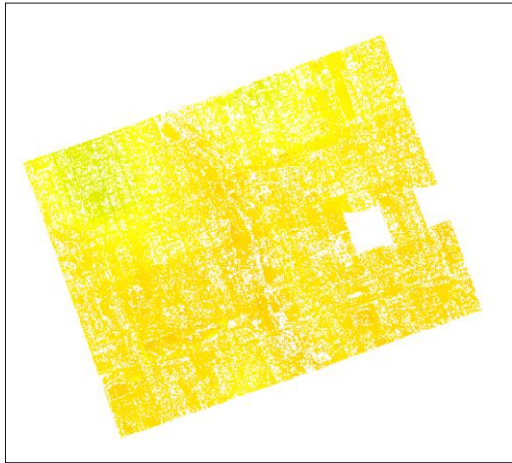
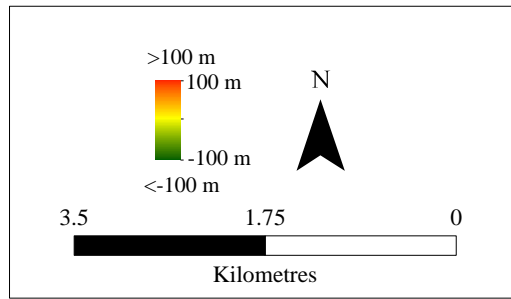
In the case of the ASTER-17 and Landsat 8 Multispectral-29 DEM, the high level of error may potentially be attributed to the incorrect detection and location of matched points between the images. This potentially occurred due to the large difference in spatial resolution between the two images, with the ASTER image having a resolution of 15 m and Landsat 8 having a resolution of 30 m.

In the case of the ASTER-18 and Bing Maps DEM, the spatial resolution was matched closely at 15 m for the ASTER image, and 13 m for the Bing Maps image. However, the large error would potentially have also originated with a failure to correctly match points between the two images. This may be because the Bing Maps images are aerial images that have been mosaiced together, causing geometric differences among matched points. Also, Bing Maps images may have undergone post-processing enhancements or radiometric corrections, making features appear different between the two images.

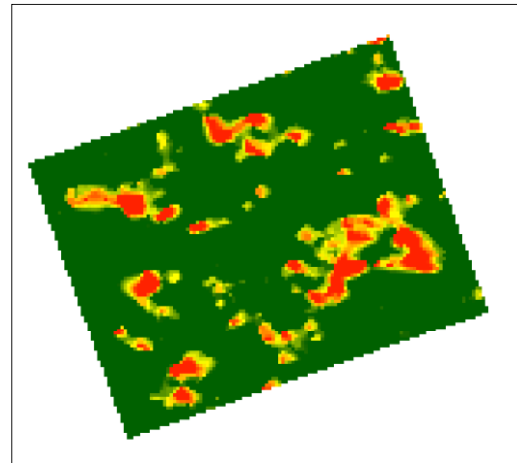
4.3 Differenced Digital Elevation Model Results

The accuracy assessment provided a means to statistically compare the generated DEMs, however the twenty-five control points used over the 6.633 km² study area may not have provided a sufficiently sized sample. To compensate for this, and to compliment the accuracy assessment, the seven generated DEMs were differenced with the control DEM from the Ministry of Natural Resources to visually assess errors in elevation.

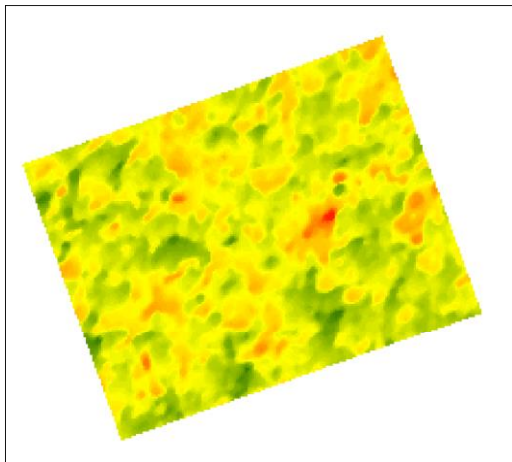
These differenced models are depicted in Figure 7, on the following pages, and represent the result of subtracting the control DEM raster from the generated DEM raster. Interpreting the results, the closer the resulting differenced raster value is to zero, the smaller the bias. The models in Figure 7 are represented in the same scale, for the sake of comparison. (The same models, represented in unique scales based on each model's maximum and minimum value, may be seen in the Appendix, Figure 11).



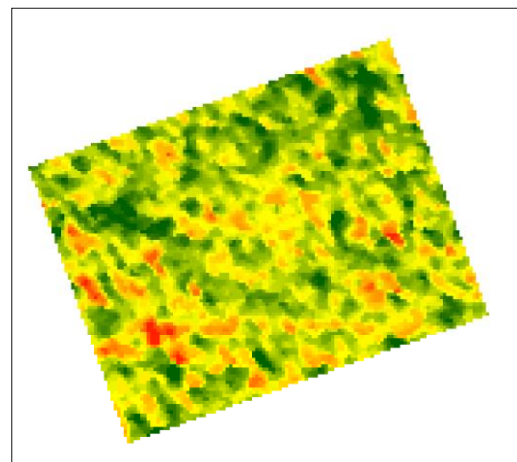
Differenced Aerial



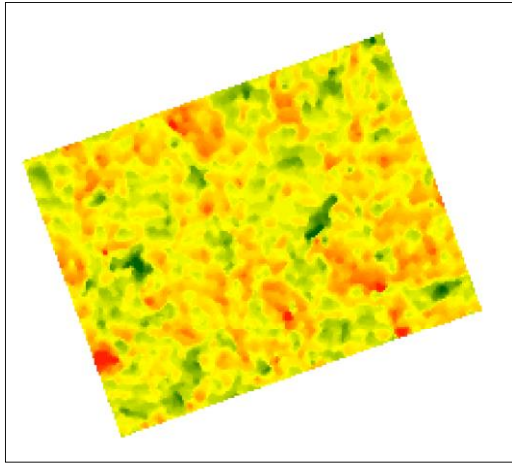
Differenced ASTER-17 and Landsat 8
Multispectral-29



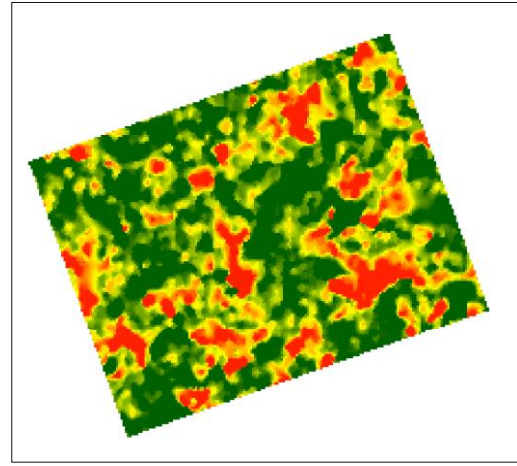
Differenced Sentinel and Landsat 8
Multispectral-29



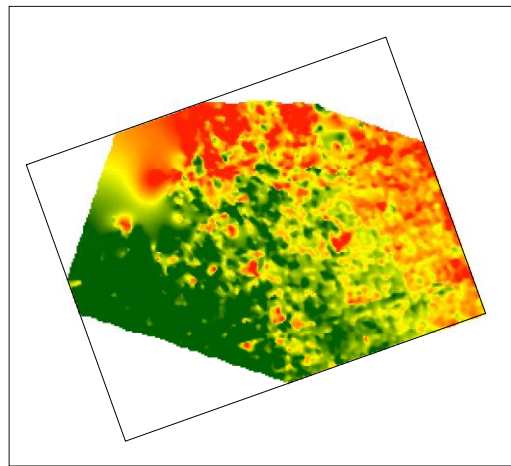
Differenced Sentinel and Landsat 8
Multispectral-30



Differenced Sentinel and ASTER-17



Differenced Sentinel and ASTER-18



Differenced ASTER-18 and Bing Maps

Figure 7 - Generated DEMs differenced with the control DEM from the Ministry of Natural Resources. The models are represented in the same scale of elevation error, for comparison.

From visual inspection of the errors, it is clear that the trend observed from the accuracy assessment is maintained. The DEM with the least amount of error is the DEM generated from aerial images. Following the aerial images, both the DEM generated from Sentinel and Landsat 8 Multispectral-29 and the DEM generated from Sentinel and ASTER-17, appear to have a relatively low level of error, confirming the rankings of RMSE values of 20.579 m and 20.047 m, respectively.

Also following the levels of error seen in the accuracy assessment, the Sentinel and Landsat 8 Multispectral-30 DEM has more error than the three previously mentioned DEMs, followed by the DEM generated using Sentinel and ASTER-18. However, these levels of error appear not to reach the extremes of the remaining two DEMs. The remaining two DEMS being ASTER-17 and Landsat 8 Multispectral-29, and ASTER-18 and Bing Maps, which produced the highest RMSE, also visually produce the most erroneous differenced rasters.

5 DISCUSSION

5.1 Effects of Resolution on Digital Elevation Models

Besides the seven DEMs that were generated, there were twenty possible image pairs that failed to generate DEMs. Each unsuccessfully generated DEM failed at the feature detection stage of the process, meaning that common features between images were not found. Since there is significant overlap among all the images (29% overlap between ASTER-17 and ASTER-18 being the least amount), the issue was not that there were no coincident features between image pairs. This suggests that varying spatial resolution is one potential cause of failure.

The clearest case of this is with that of the aerial images, which failed to generate DEMs with every other image. The aerial images have a spatial resolution of 0.07 m, which is very different from that of the satellite images, with the ASTER images having the closest spatial resolution at 15 m. This meant that features in both images appeared very differently and thus the feature detection algorithm was unable to generate matching points between images.

However, when combining the aerial images with images from Bing Maps, with spatial resolutions of 0.07 and 0.15 m, respectively, the feature detection failed. This was possibly due to the images being taken in different seasons, or due to the mosaicking of the aerial images, or various radiometric corrections applied to the Bing Maps images before publication.

Large differences in spatial resolutions may also explain the reason why the Landsat 8 Multispectral images, with spatial resolution of 30 m, failed to generate DEMs with ASTER-18, Landsat 8 Panchromatic images, and the aerial images, which all have spatial resolutions of 15 m or less. And when Landsat 8 Multispectral-29 was able to generate a DEM with ASTER-17, it produced the highest RMSE value, 236.094 m. This suggests that for successful DEM generation, the difference in spatial resolution of the image being used must not exceed 15 m, or must stay within 10 m.

The observation that similar spatial resolutions between images may also explain why the Sentinel image was successfully able to generate DEMs with each of the ASTER and Landsat 8 Multispectral images. The Sentinel image spatial resolution of 20 m was relatively close to both the ASTER and Landsat 8 Multispectral image resolutions of 15 m and 30 m, respectively. These results produced the best RMSE values of the DEMs generated from the open sources images.

However, there were cases observed where similar or exact spatial resolutions between image pairs failed to generate DEMs. This is evident in the case of the Landsat 8 Panchromatic images, of spatial resolution 15 m, which failed to generate DEMs with the ASTER images and the Sentinel image, or spatial resolutions 15 m and 20 m, respectively. Though the spatial resolutions were either exactly the same or close, features failed to match. This is thought to be due to the difference in radiometry between the images, and is discussed in the following section.

One way to overcome the limitation of requiring images of similar resolutions is down sampling. With down sampling, an image of fine resolution undergoes an image scaling so that its resolution is made coarser, potentially matching the resolution of another coarse image with which a DEM may be generated. The failed DEM combinations in this study all occurred at the feature matching phase. Down sampling would potentially make features in fine resolution images lose detail and appear as they do in coarser resolution images. This may overcome the failure of feature matching.

Popular methods of resampling include Nearest-Neighbour, Bilinear and Bicubic interpolation methods. Each has benefits and drawback with respect to the preservation of spatial information, which is key in feature matching, as is discussed by Xiong & Zhang (2010).

An alternative to down sampling is the process of panchromatic sharpening, or “pansharpening”. With pansharpening, a coarse resolution multispectral image would be made finer in resolution by fusing it with a fine resolution panchromatic image. This could potentially allow for successful feature matching with fine resolution images and allow for DEMs to be generated.

There are various methods of pansharpening, including Gram-Schmidt spectral sharpening and many wavelet-based methods. Different methods have considerations to be made with respect to spectral and spatial information preservation, as is described by Vivone et al. (2015).

5.2 Effects of Radiometry on Digital Elevation Models

As has been discussed, it is important that the spatial resolution of images used to generate DEMs be relatively similar for accurate results (within a 10 m difference between pairs of satellite

images). And as has also been discussed, the radiometry of the images being used must be similar as well, and is crucial for DEM generation.

The clearest example of this is the failure of the Landsat 8 Panchromatic images to generate any DEMs when paired with other images. The Landsat 8 Panchromatic images have a spatial resolution of 15 m, exactly that of the ASTER images, and similar to that of the Sentinel image (20 m), yet it still failed to generate DEMs. This is believed to be due to the images intensity and contrast.

The Landsat 8 Panchromatic images have a lower brightness and higher contrast than the other images that were paired with them. This made features in the image appear much differently compared to the other images. When features appear differently, tie points fail to generate, potentially explaining why the Panchromatic images failed at the feature matching phase, when paired with every other image.

The observation of requiring similar radiometry is also seen with the images from Bing Maps. The images from Bing Maps appear to have undergone some form of radiometric corrections, and is likely the cause of the failure at the feature detection phase as well. Even though spatial resolutions were kept similar to those of the image being paired with.

A way to potentially overcome differing radiometric properties in image pairs is radiometric equalization or normalization. In the process of radiometric equalization, the statistical properties of radiometric information of a pair of overlapping images are considered. The properties are determined either for the entire overlapping area, or for certain smaller areas. The statistical properties are used to correct the brightness offset, contrast, and intensity or gain of either one of both images, such that the result is similar radiometry between the pair. A more detailed investigation of the types and effects of radiometric equalization is discussed by Du et al. (2001).

6 CONCLUSION

The aim of this project was to determine if DEMs generated using open source images could compare, or even surpass, the vertical accuracies of freely available DEMs, such as ASTER GDEM, SRTM GDEM, or EarthEnv-DEM90. To do this, images from ASTER, Landsat 8, Sentinel-2, and Bing Maps were used in pairs to generate DEMs over Oshawa, Canada. These images were selected for their open source nature and for their varying spatial resolution. Aerial images were also included, for comparison. There were twenty-seven potential pairings of images that could produce DEMs.

Of the possible twenty-seven DEMs, seven were successfully generated, and twenty failed to generate. The successfully generated DEMs had spatial resolutions that were approximately that of the images with coarser resolution between the pairs used to generate them. This was true for all generated DEMs, except for the one generated using Landsat 8 Multispectral-29 and Sentinel, which had a 20 m spatial resolution, matching that of the finer resolution Sentinel image and not the coarser image, Landsat 8 (30 m).

It was also found that the greatest factor contributing towards the success of DEM generation was the difference in spatial resolution between image pairs. Image pairs with large differences in spatial resolution failed to generate DEMs. Specifically, these pairs failed at the feature matching phase. This would be due to features being represented very differently between images pairs of large resolution differences.

Alternatively, when images were of similar spatial resolutions, DEMs were successfully generated with relatively high accuracies. The lowest RMSE values of all of the generated DEMs were 20.047 m and 20.579 m, made when combining images from the Sentinel-2 satellite with images from the ASTER and Landsat 8 sensors, respectively. Sentinel images, with a resolution of 20 m, had the most success in generating DEMs with other satellite images, because of its similarity to images with resolutions of 15 m and 30 m. It was found that DEMs were able to be generated with relatively high accuracy when the difference between resolutions of image pairs was within 10 m.

It was also observed that radiometry is required to be similar between image pairs. This was found to be the reason that the low-intensity, high-contrast Landsat 8 Panchromatic images, though similar in spatial resolution to other images, failed to generate any DEMs. Comparable radiometry,

similar to the need for similar spatial resolutions, allowed for feature detection to occur more successfully in DEM production.

In conclusion, the project was not able to consistently generate DEMs of accuracies that surpass those of other open source datasets. However, in certain cases, DEMs were produced that did exceed the vertical accuracy of some open source datasets. It was found that elevation accuracies are proportional with image resolution, thus, using open source images with spatial resolutions finer than 15 m may potentially exceed the accuracies of the open source DEMs.

APPENDIX

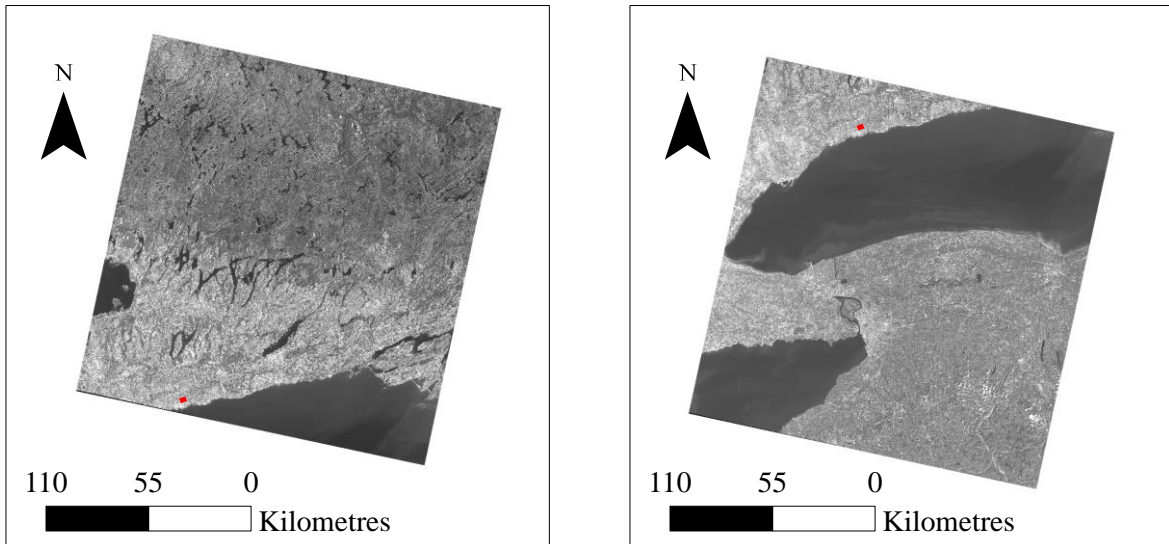
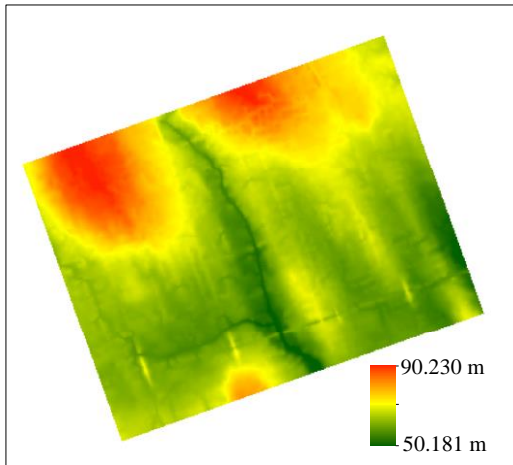


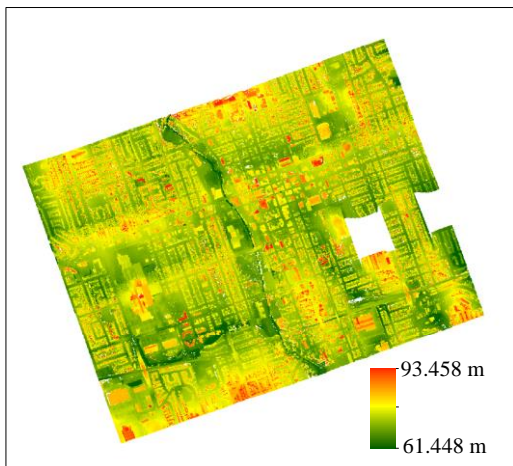
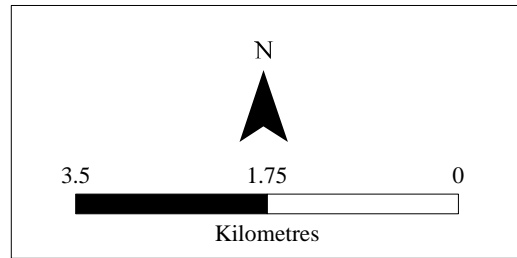
Figure 8 - Landsat 8 Panchromatic-29 (left) and Landsat 8 Panchromatic-30 (right), with study area is marked in red. The images are numbered for their WRS Row Number.



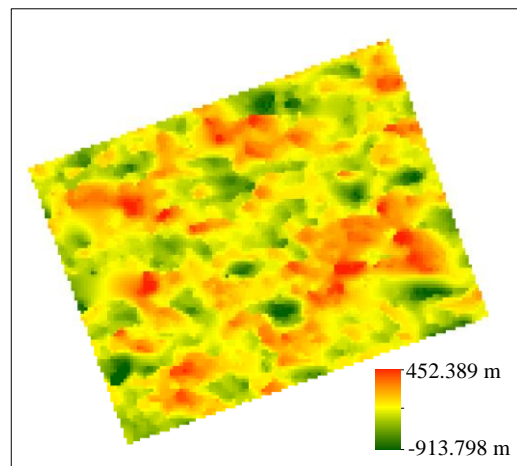
Figure 9 – Bing Maps Images, with resolutions 0.15 m (left), 13 m (centre), and 27 m (right).



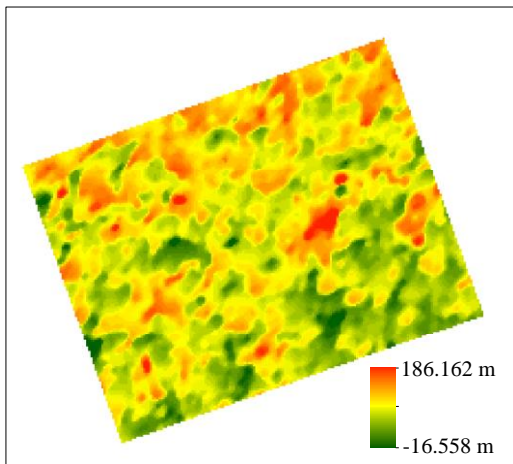
Ontario Ministry of Natural Resources



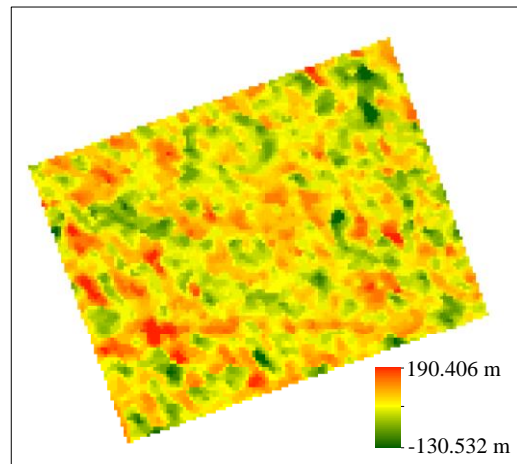
Aerial Images



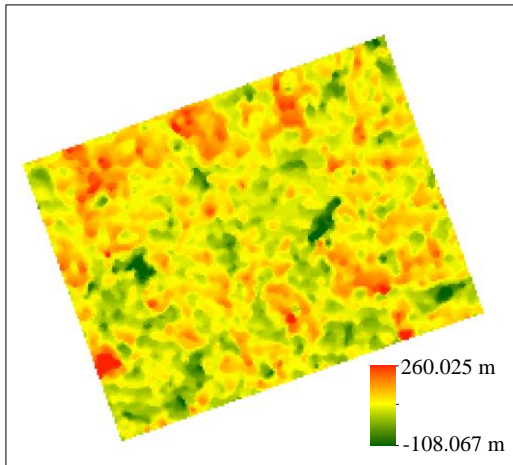
ASTER-17 and Landsat 8 Multispectral-29



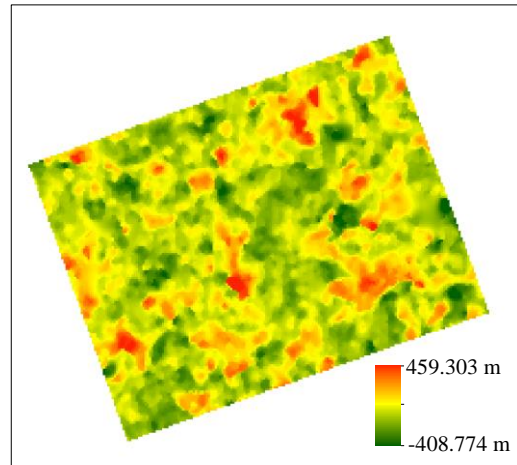
Sentinel and Landsat 8 Multispectral-29



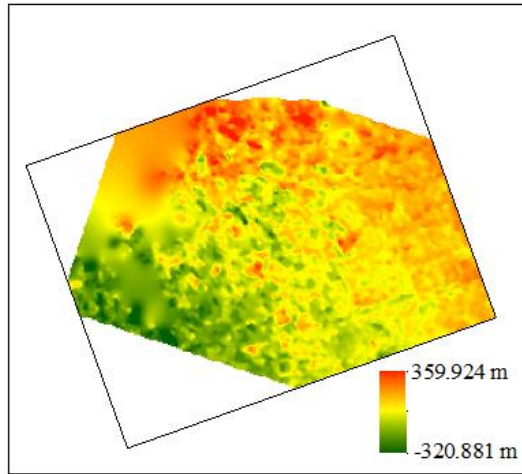
Sentinel and Landsat 8 Multispectral-30



Sentinel and ASTER-17



Sentinel and ASTER-18

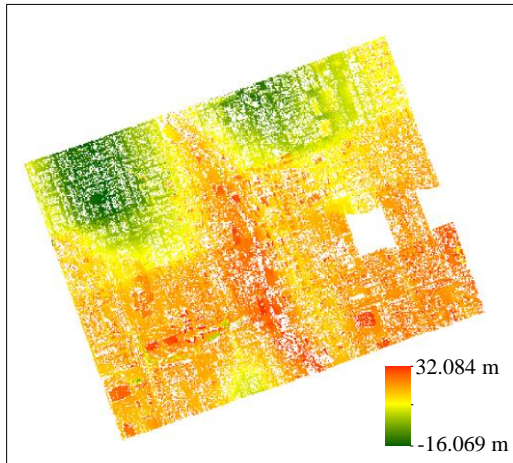


ASTER-18 and Bing Maps

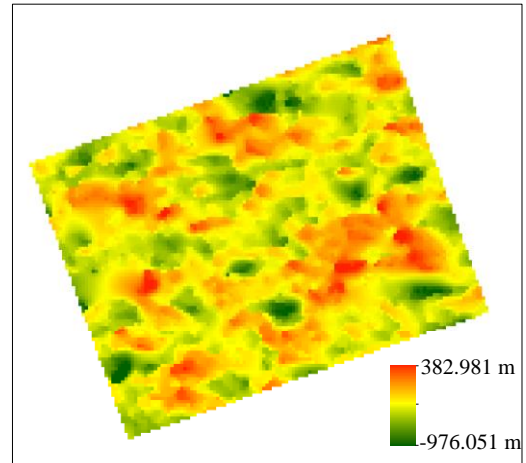
Figure 10 - The seven DEMs that were generated, identified by image pairs used to generate them, with the Ontario Ministry of Natural Resources DEM at the top, for reference.

Ground Control Points				Elevations (m)							
ID	Eastings	Northings	Control Height	Ministry of Natural Resources	Aerial Images	Generated Digital Elevation Models					
						ASTER-17 & Landsat 8-29	Sentinel & Landsat 8-29	Sentinel & Landsat 8-30	Sentinel & ASTER-17	Sentinel & ASTER-18	ASTER-18 and Bing Maps
ASC_200	670138.5439	4860639.635	71.7331	66.912	80.152	-416.043	73.268	78.931	49.261	-47.889	N/A
ASC_201	670718.5891	4860945.472	66.3268	62.043	75.780	-17.931	65.117	62.258	49.317	-71.532	N/A
ASC_202	671257.966	4861120.243	72.5716	69.289	78.394	-118.171	35.536	23.092	88.568	244.065	-86.053
ASC_203	670925.6369	4861449.019	63.7917	59.095	72.620	-237.948	48.771	106.248	53.018	76.384	-112.790
ASC_204	671974.9219	4861492.511	72.046	67.381	78.624	-92.374	47.731	28.778	83.653	-13.362	10.754
ASC_205	669940.3275	4861637.095	68.5713	64.306	77.515	-160.145	42.853	-3.541	65.017	4.511	-188.155
ASC_206	670612.9684	4861643.316	66.7651	61.337	77.641	-6.020	96.431	61.940	31.774	101.813	-126.241
ASC_207	671231.3787	4861620.104	65.1027	60.721	76.215	37.820	65.190	67.727	78.118	79.980	-60.905
ASC_208	670863.2104	4862003.015	68.8374	64.197	78.216	-122.469	39.456	8.812	73.983	43.873	-74.465
ASC_209	670902.5967	4862592.586	70.8032	66.608	79.524	-178.863	69.634	113.374	89.510	21.498	-26.010
ASC_213	670723.8442	4863131.842	70.5229	66.035	76.443	-68.584	84.859	-43.668	55.908	-52.171	177.708
ASC_214	671340.0029	4863160.521	77.8215	73.269	76.637	110.906	79.011	52.028	78.109	86.141	236.777
ASC_100	671143.5853	4862875.146	70.2164	65.639	76.522	-558.766	56.925	45.184	66.223	71.639	181.112
ASC_101	672213.8083	4863240.94	74.9862	70.230	76.790	-169.551	82.932	57.099	64.626	-105.258	53.264
ASC_102	672606.9548	4862277.67	66.255	62.792	N/A	1.997	48.768	86.353	103.397	19.784	55.268
ASC_103	671592.5145	4861980.052	66.4692	61.698	76.225	9.427	62.417	36.728	109.965	-8.433	26.198
ASC_104	671236.1308	4862460.146	62.8613	57.923	74.410	-172.427	47.704	97.552	71.873	26.272	-191.945
ASC_105	670245.8187	4861380.553	67.0172	61.578	75.507	15.985	54.959	33.327	105.691	257.406	N/A
ASC_106	670113.1872	4861938.537	71.0003	66.317	75.884	-60.950	70.203	108.325	71.978	79.350	-118.682
ASC_107	669915.0284	4862465.919	86.5187	82.750	75.758	-46.222	65.443	3.977	98.035	-80.466	-2.663
ASC_108	670024.0527	4862479.393	87.4502	83.873	76.038	-101.069	35.276	-11.550	92.769	-34.434	40.642
ASC_109	670060.2668	4862367.5	84.8539	80.289	79.926	-124.482	89.179	48.488	96.370	-40.706	-4.299
ASC_110	670079.8939	4862314.761	82.863	78.895	79.525	-215.099	83.824	55.877	105.629	-50.742	-116.503
ASC_111	669985.6423	4862265.542	78.4647	74.532	79.147	-162.812	53.695	18.768	71.145	-11.443	-46.054
ASC_112	669926.9431	4862359.296	82.0197	77.374	79.624	-102.730	49.701	56.235	112.212	61.575	-22.315

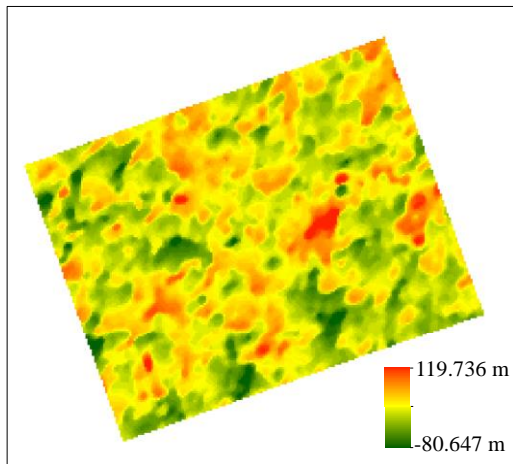
Table 4 – The elevation of the DEMs at the location of the control points, along with control elevation. All elevations are with respect to the datum, WGS 1984.



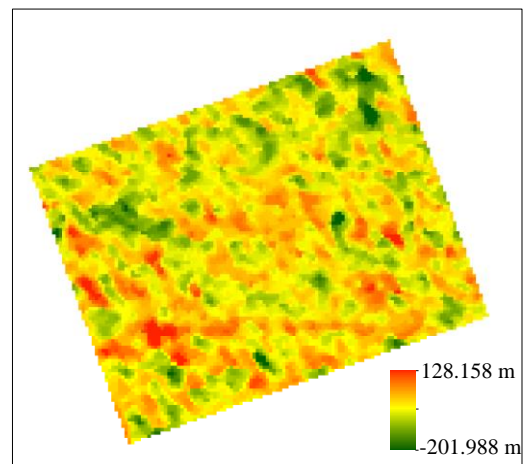
Aerial Images



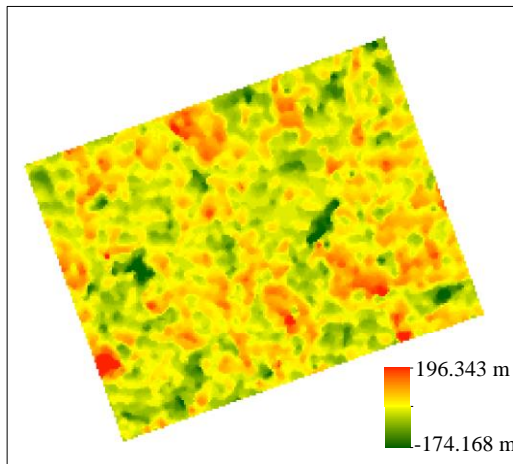
ASTER-17 and Landsat 8 Multispectral-29



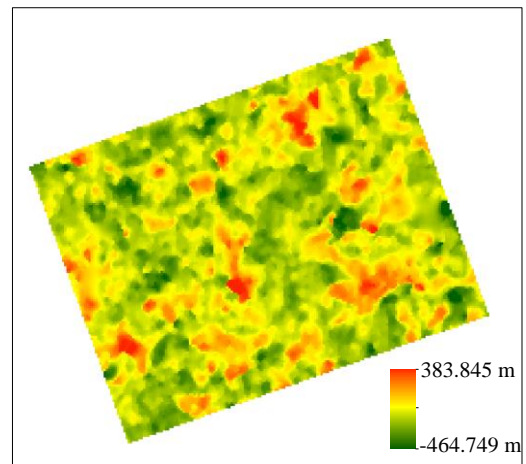
Sentinel and Landsat 8 Multispectral-29



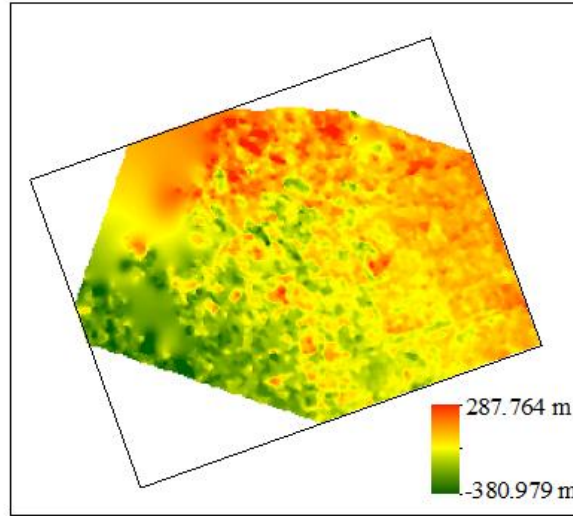
Sentinel and Landsat 8 Multispectral-30



Sentinel and ASTER-17



Sentinel and ASTER-18



ASTER-18 and Bing Maps

Figure 11 - Generated DEMs differenced with the control DEM from the Ministry of Natural Resources, represented in unique scales.

REFERENCES

1. Du, Y., Cihlar, J., Beaubien, J., & Latifovic, R. (2001). Radiometric normalization, compositing, and quality control for satellite high resolution image mosaics over large areas. *IEEE Transactions on Geoscience and Remote Sensing*, 39(3), 623-634. doi:10.1109/36.911119
2. Hirt, C., Filmer, M. S., & Featherstone, W. E. (2010). Comparison and validation of the recent freely available ASTER-GDEM ver1, SRTM ver4.1 and GEODATA DEM-9S ver3 digital elevation models over Australia. *Australian Journal of Earth Sciences*, 57(3), 337-347. 10.1080/08120091003677553
3. Li, P., Shi, C., Li, Z., Muller, J., Drummond, J., Li, X., . . . Liu, J. (2013). Evaluation of ASTER GDEM using GPS benchmarks and SRTM in china. *International Journal of Remote Sensing*, 34(5), 1744-1771. 10.1080/01431161.2012.726752
4. Li, X., Zhang, X., Zhang, Y., Jin, X., & He, Q. (2017). Comparison of digital elevation models and relevant derived attributes. *Journal of Applied Remote Sensing*, 11(4), 046027-046027. 10.1117/1.JRS.11.046027
5. National Aeronautics and Space Administration, Jet Propulsion Laboratory (2001). SRTM Mission Statistics. Page 1. Retrieved from <https://www2.jpl.nasa.gov/srtm/statistics.html>
6. METI (Japanese Ministry of Economy, Trade and Industry, National Aeronautics and Space Administration, United States Geological Survey (2009). ASTER Global DEM Validation Summary Report. Page 2. Retrieved from https://lpdaac.usgs.gov/sites/default/files/public/aster/docs/ASTER_GDEM_Validation_Summary_Report.pdf
7. Rayburg, S., Thoms, M., & Neave, M. (2009). A comparison of digital elevation models generated from different data sources. *Geomorphology*, 106(3), 261-270. 10.1016/j.geomorph.2008.11.007
8. Risbøl, O., Briese, C., Doneus, M., & Nesbakken, A. (2015). Monitoring cultural heritage by comparing DEMs derived from historical aerial photographs and airborne laser scanning. *Journal of Cultural Heritage*, 16(2), 202-209. 10.1016/j.culher.2014.04.002
9. Robinson, N., Regetz, J., & Guralnick, R. P. (2014). EarthEnv-DEM90: A nearly-global, void-free, multi-scale smoothed, 90m digital elevation model from fused ASTER and

- SRTM data. *ISPRS Journal of Photogrammetry and Remote Sensing*, 87, 57-67.
10.1016/j.isprsjprs.2013.11.002
10. Sharma, A., Tiwari, K. N., & Bhadoria, P. B. S. (2011). Determining the optimum cell size of digital elevation model for hydrologic application. *Journal of Earth System Science*, 120(4), 573-582. 10.1007/s12040-011-0092-3
 11. Vivone, G., Alparone, L., Chanussot, J., Dalla Mura, M., Garzelli, A., Licciardi, G. A., Russo, R., Wald, L. (2015). A critical comparison among pansharpening algorithms. *IEEE Transactions on Geoscience and Remote Sensing*, 53(5), 2565-2586. doi:10.1109/TGRS.2014.2361734
 12. Xiong, Z., & Zhang, Y. (2010). A critical review of image registration methods. *International Journal of Image and Data Fusion*, 1(2), 137-158. doi:10.1080/19479831003802790
 13. Yang, L., Meng, X., & Zhang, X. (2011). SRTM DEM and its application advances. *International Journal of Remote Sensing*, 32(14), 3875-3896. 10.1080/01431161003786016